SF2A 2023
M. N'Diaye, A. Siebert, N. Lagarde, O. Venot, K. Baillié, M. Béthermin, E. Lagadec, J. Malzac, J. Richard (eds)

THE COSMOLOGICAL POTENTIAL OF HIGH-REDSHIFT CLUSTERS WITH DEEP X-RAY SURVEYS

N. Cerardi[1], M. Pierre[2], P. Valageas[3] and C. Garrel[4]

Abstract.

Since 2022, the ATHENA mission, selected in the ESA's Cosmic Vision Program, is undergoing a deep redefinition process due to budgetary constraints. However, in its current scope, this X-ray satellite is poised to unveil the high-z population of galaxy clusters with an unprecedented sensitivity compared to current telescopes. The high redshift population of clusters is a key lever arm to understand the evolution of dark energy - a goal that is complementary to many upcoming ground and space-based extragalactic surveys.

We consider two surveys designs to be carried out by the Wide Field Imager (WFI) of ATHENA, deriving simplified selection functions for both cases. Up to $z \sim 2$, we expect to recover thousands of clusters down to the low-mass (group) scale. We then perform a forward modelling of the theoretical cluster number counts into X-ray observable diagrams. We present cosmological forecasts for different cosmologies, emphasising the detection of high-z clusters will be crucial in obtaining independent constraints on dark energy. Such measurements with X-ray selected samples will only be possible with the launch of ATHENA in the 2030s.

Keywords: X-ray: galaxies: clusters, Cosmological parameters, Fisher forecasts

1 Introduction

At both early and late times, open questions remain in cosmology and challenge the standard cosmological model, namely ΛCDM. The recent and upcoming observatories (such as eROSITA, JWST, Euclid, Vera Rubin, CMB-S4...) are poised to bring a physical understanding on the natures of Dark Matter and Dark Energy (DE), as well as studying the inflation era.

Clusters of galaxies lie on the nodes of the cosmic web and as such are tracers of both the expansion of the Universe and the growth of structures. Therefore they naturally appear as cosmological probes, either through their number counts, their spatial clustering, or their gas fraction. The Halo Mass Function (HMF), used in number counts studies is particularly sensitive to Ω_m and σ_8 (see for instance Garrel et al. 2022). At high redshift, the sensitivity of the cluster population to the DE Equation of State (EoS) and to primordial non Gaussianities is increased (Majumdar & Mohr 2004; LoVerde et al. 2008). Galaxy cluster samples so far are restricted to the most massive end of the distribution, or to low-redshifts ($z < 1$). The next generation X-ray telescope ATHENA, to be launched in the late 2030s, is expected to reach unprecedented sensitivity. It will carry onboard a Wide Field Imager (WFI, Meidinger et al. 2017), able to run deep extragalactic X-ray surveys.

This study presents the forecasts for deep X-ray surveys achievable by ATHENA/WFI. We derive analytical selection functions and forecast the number of clusters to be detected. We furthermore study the cosmological potential of such samples by running a Fisher analysis, for the DE EoS and primordial non-Gaussianities. This work is extensively developped in Cerardi et al., 2023 (submitted).

[1] Université Paris Cité, Université Paris-Saclay, CEA, CNRS, AIM, F-91191, Gif-sur-Yvette, France
[2] Université Paris-Saclay, Université Paris Cité, CEA, CNRS, AIM, 91191, Gif-sur-Yvette, France
[3] Institut de Physique Théorique, Université Paris-Saclay, CEA, CNRS, F-91191 Gif-sur-Yvette Cedex, France
[4] Max Planck Institute for Extraterrestrial Physics, Giessenbachstrasse 1, D-85748 Garching, Germany

Survey	Area (deg^2)	Depth (ks)	Nb of clusters in $0 < z < 2$	Nb of clusters in $1 < z < 2$
A	50	80	5500	940
B	200	20	11200	1400

Table 1. Survey designs modelled in this work. A and B share the same total exposure time ($\approx 9Ms$ for ATHENA/WFI).

2 Cluster population modelling

2.1 Cosmology

To model the cluster population, we take as fiducial cosmology the flat ΛCDM model with the values of Planck Collaboration et al. (2020). As ATHENA will operate in the late 2030s, we give Planck priors on h, Ω_b and n_s. We also want to test the constraining power of ATHENA on extensions of the standard model. In a first case, we write the DE EoS in the form $p/(\rho c^2) = w(a) = w_0 + w_a(1-a)$. In a second case, we consider deviations from Gaussianity in the primordial perturbation field. We focus here on non-Gaussianities of the local type, where the Bardeen potential is then expressed at lowest order with a quadratic term, parametrized by : $\Phi(x) = \phi(x) + f_{NL}^{loc}\left[\phi(x)^2 - \langle\phi\rangle^2\right]$. ϕ is a Gaussian field and f_{NL}^{loc} captures the amplitude of the non-Gaussian deviation. Followingly, cluster abundance is modelled following the HMF from Tinker et al. (2008).

2.2 Scaling relations

To convert the cluster mass* into ICM luminosity and temperature, we use the scaling relations formalism derived from XXL with HSC (Hyper Suprime-Cam) weak-lensing masses. We keep the slopes of the $T-M$ and $L-M$ fits from Sereno et al. (2020). The evolution parameters are set to self similarity, and the normalisations are refitted alone on the XXL C1 catalogue to ensure that (i) we recover the correct C1 number counts and (ii) it compensates for the weak-lensing mass bias.

We then transform the luminosity and temperature properties into count-rates, we assume throughout our study that the sensitivity of the ATHENA/WFI is equivalent to be five times that of XMM/EPIC(pn+mos1+mos2). We use the APEC model with the AtomDB database (Smith et al. 2001), and the response files of XMM/EPIC instruments to obtain the count-rate (CR) in the band [0.5–2] keV and the hardness-ratio (HR), the ratio of the count-rates in [1–2] keV and in [0.5–1] keV.

3 Detected cluster population

We then consider two survey designs that share the same exposure time ∼9 Ms. The first one, survey A, spans 50 deg^2 with a depth of 80ks, and the second one, survey B, is 4 times wider but 4 times shallower. In the band of interest, the particle background is assumed to be 2.5×10^{-7} c/s/arcsec^2, and the diffused X-ray backround is assumed to be the XMM one scaled to the ATHENA sensitivity: 4.08×10^{-6} c/s/arcsec^2. We then compute the completeness for both surveys, assuming that we detect clusters with a S/N ≥ 5 in a fixed aperture.

The so-defined selection functions are represented in the left panel of figure 1. At $z > 1$, ATHENA will detect clusters down to $2\times10^{13}\mathrm{h}^{-1}\mathrm{M}_\odot$ ($3.5\times10^{13}\mathrm{h}^{-1}\mathrm{M}_\odot$) for survey A (survey B), a population that will remain unprobed until ATHENA is launched. Combined with our fiducial cosmology, we can then forecast the expected number counts. The total numbers are given in table 1, and the right panel in figure 1 shows the distribution of these population as a function of redshift.

4 Cosmological forecasts

We derive cosmological forecasts for surveys A and B using a Fisher analysis. Assuming that the observations (i) are independant and (ii) follow a Poisson distribution, we can compute the Fisher matrix terms by :

$$F_{\alpha\beta} = \sum_i \frac{1}{\lambda_i}\frac{\partial\lambda_i}{\partial\theta_\alpha}\frac{\partial\lambda_i}{\partial\theta_\beta} \tag{4.1}$$

*here defined as $M_{500c} = 4\pi R_{500c}^3 500\rho_c/3$

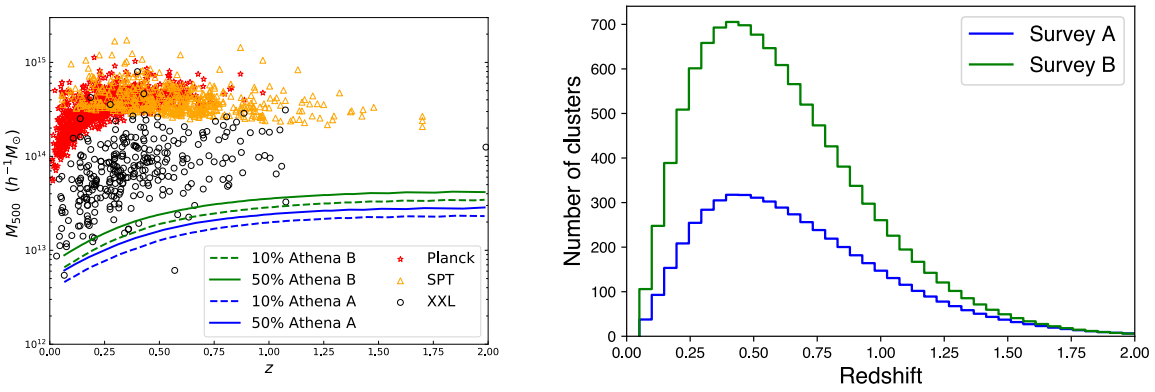

Fig. 1. Left: Mass detection limit for surveys A and B. The plain (dashed) lines represent the 50% (10%) detection limit in the $M_{500c} - z$ plane. A given cluster with mass above (resp. below) a line have a detection probability higher (resp. lower) than 50% in the corresponding survey design. The circles, stars and triangles denotes cluster samples from XXL (Adami et al. 2018), Planck SZ (Planck Collaboration et al. 2016) and SPT (Bleem et al. 2015), respectively. **Right:** Number counts for surveys A and B. Survey A has a density of clusters that is about twice the density in B, but the effect of the survey area dominates and B detects twice as many clusters as A (11200 vs 5500).

case	survey	$\Delta\Omega_m$	$\Delta\sigma_8$	Δw_0	Δw_a	Δf_{NL}
w_zCDM	A	0.025	0.015	0.32	1.25	
	B	0.016	0.0091	0.22	0.87	
Local primordial non Gaussianity	A	0.014	0.038			470
	B	0.0094	0.025			310

Table 2. Constraints derived from the Fisher analysis. 9 supplementary parameters (h, Ω_b, n_s, α_{TM}, β_{TM}, γ_{TM}, α_{LM}, β_{LM}, γ_{LM}) are included in the analysis and marginalised. The results quoted are the 1σ uncertainties, in $0.05 < z < 2$.

Inversing the Fisher matrix gives access to the covariance, hence the best achievable constraints. We always include in our analysis five cosmological parameters: Ω_m, σ_8, h, Ω_b, n_s; and 6 parameters of the T-M and L-M scaling relations: α_{TM}, β_{TM}, γ_{TM}, α_{LM}, β_{LM}, γ_{LM}. Given that Ω_m and σ_8 strongly influence cluster abundances, these parameters have no prior. We then provide cosmological forecasts either for the w_zCDM scenario, adding w_0 and w_a; or with primordial local non Gaussianities and the parameter f_{NL}^{loc}.

4.1 Forecasted constraints for surveys A and B

In table 2 we present the results of the Fisher analysis for each survey and each cosmological test. The results are marginalised over h, Ω_b, n_s and the scaling relations parameters. Thanks to its larger statistics, survey B outperforms survey A in all scenarii by a factor ≈1.4.

4.2 Impact of the high redshift counts

We now study the contribution of clusters at $z > 1$ in the analysis. We here focus on survey B as it is the most powerful survey, as seen in the previous section. We operate successives redshift-truncated analysis, as shown in figures 2 and 3, respectively for w_zCDM and local primordial non-gaussianities. In each panel, the outer-most ellipse encompasses $0.05 < z < 1$. The inner ellipses sequentially include the 5 remaining bins in the Fisher analysis. In each configuration, we observe that high-z bins induce a tilt of the ellipse, reducing the uncertainty for these parameters. Clusters at $z > 1$ only represents $\sim 15\%$ of the total sample, so that their statistical effect is not dominant. However, they help to break the degeneracy between parameters within the cluster abundance analysis for $z < 1$. This effect is very strong in the plane w_0–w_a: Δw_a shrinks by a factor ∼2.3. The same trend is observed for local primordial non-Gaussianities: clusters in $1 < z < 2$ improve the constraints on f_{NL}^{loc} by a factor ~ 2.6.

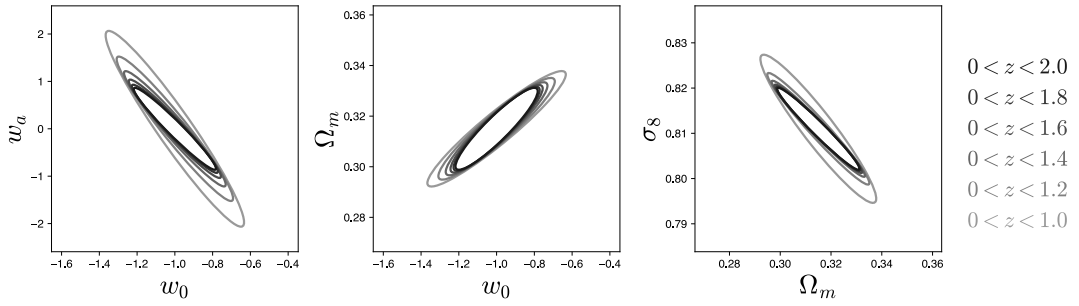

Fig. 2. w_zCDM

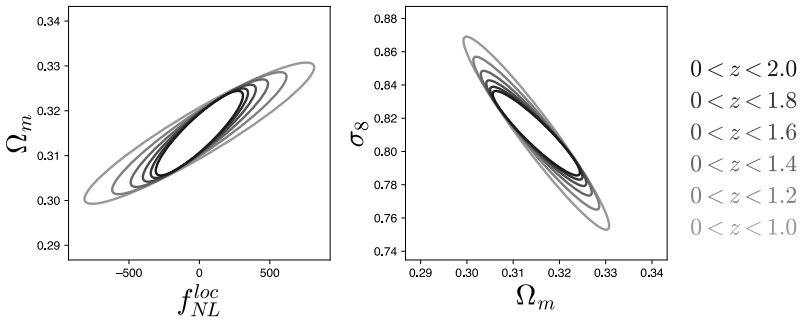

Fig. 3. Local primordial non Gaussianities

5 Conclusions

We studied the potential of high redshift clusters with deep X-ray surveys to be achieved by an ATHENA-like observatory. For two different survey designs, we derived selection functions and expected number counts for these surveys. The detected clusters populate a range of mass and redshift unprecedented with X-ray telescopes, up to $z \sim 2$. They contain critical cosmological information and breaks the degeneracy between parameters. High-redshift clusters are hence shown to be a very important component of the DE investigations. Their detection will require a powerful X-ray telescope of new generation such as ATHENA.

References

Adami, C., Giles, P., Koulouridis, E., et al. 2018, Astronomy & Astrophysics, 620, A5, arXiv:1810.03849 [astro-ph]

Bleem, L. E., Stalder, B., de Haan, T., et al. 2015, The Astrophysical Journal Supplement Series, 216, 27, arXiv:1409.0850 [astro-ph]

Garrel, C., Pierre, M., Valageas, P., et al. 2022, Astronomy & Astrophysics, 663, A3, arXiv:2109.13171 [astro-ph]

LoVerde, M., Miller, A., Shandera, S., & Verde, L. 2008, Journal of Cosmology and Astroparticle Physics, 2008, 014, arXiv:0711.4126 [astro-ph]

Majumdar, S. & Mohr, J. J. 2004, The Astrophysical Journal, 613, 41, publisher: IOP Publishing

Meidinger, N., Eder, J., Eraerds, T., et al. 2017, The Wide Field Imager Instrument for Athena, arXiv:1702.01079 [astro-ph]

Planck Collaboration, Ade, P. A. R., Aghanim, N., et al. 2016, Astronomy & Astrophysics, 594, A27, arXiv:1502.01598 [astro-ph]

Planck Collaboration, Aghanim, N., Akrami, Y., et al. 2020, Astronomy & Astrophysics, 641, A6, arXiv:1807.06209 [astro-ph]

Sereno, M., Umetsu, K., Ettori, S., et al. 2020, Monthly Notices of the Royal Astronomical Society, 492, 4528, arXiv:1912.02827 [astro-ph]

Smith, R. K., Brickhouse, N. S., Liedahl, D. A., & Raymond, J. C. 2001, The Astrophysical Journal, 556, L91, publisher: IOP Publishing

Tinker, J. L., Kravtsov, A. V., Klypin, A., et al. 2008, The Astrophysical Journal, 688, 709, arXiv:0803.2706 [astro-ph]